Journal of NUCLEAR SCIENCE and TECHNOLOGY, Vol. 45, No. 5, p. 390–401 (2008)

ARTICLE

Chemical Isotopic Analysis of Fission Products in PWR-MOX Spent Fuels and Computational Evaluation Using JENDL, ENDF/B, JEF, and JEFF

Akihiro SASAHARA[1,*], Tetsuo MATSUMURA[2], Giorgos NICOLAOU[3] and Yoshiaki KIYANAGI[4]

[1]*Nuclear Technology Research Laboratory, Central Research Institute of Electric Power Industry, 11-1 Iwado Kita 2-Chome, Komae-Shi, Tokyo 201-8511, Japan*
[2]*Material Science Research Laboratory, Central Research Institute of Electric Power Industry, 2-61 Nagasaka, Yokosuka-Shi, Kanagawa 240-0196, Japan*
[3]*Laboratory of Nuclear Technology, Department of Electrical and Computer Engineering, Faculty of Engineering, Democritus University of Thrace, 67100 Xanthi, Greece*
[4]*Graduate School of Engineering, Hokkaido University, Kita 13, Nishi 8, Kita-ku, Sapporo 060-8628, Japan*

(Received August 23, 2007 and accepted in revised form November 30, 2007)

A chemical isotopic analysis of high-burn-up MOX spent fuels with a burn-up of 45 MWd/kgHM was carried out to accumulate nuclide composition data. Furthermore, computational analysis was performed using the integrated burn-up calculation code system SWAT. The differences between the amounts of fission products obtained by the chemical isotopic analysis and SWAT calculation using JENDL-3.2, JENDL-3.3, ENDF/B-VI.5, ENDF/B-VI.8, JEF-2.2, and JEFF-3.0 were evaluated as the ratios of the calculated values to the experimental ones (C/E ratios). The fission products such as ^{88}Sr, ^{90}Sr, ^{106}Ru, ^{133}Cs, ^{134}Cs, and ^{135}Cs, which are gamma and decay heat sources, neutron absorption nuclides, or burn-up indicators in spent fuels, were further investigated to improve their C/E ratios using the simplified burn-up chains of fission products using JENDL-3.3; consequently, the correction values for the fission yields or capture cross sections of the fission products were estimated using sensitivity coefficients. The C/E ratios for ^{154}Eu, ^{155}Eu, ^{154}Gd, ^{155}Gd, and ^{156}Gd markedly differed among libraries. The reason for this difference was also discussed using the sensitivity coefficient and capture cross section of each fission product, which is in their main sensitive production paths.

KEYWORDS: MOX fuel, isotopic analysis, fission products, sensitivity analysis, JENDL-3.2, JENDL-3.3, ENDF/B-VI.5, ENDF/B-VI.8, JEF-2.2, JEFF-3.0

I. Introduction

Japanese electric utilities are preparing for the loading of mixed-oxide (MOX) fuels in commercial light water reactors. MOX spent fuels discharged from commercial reactors will be stored in storage facilities, when the utilization of MOX fuels progresses. Fission products accumulated in MOX spent fuels contribute to heat generation and gamma emission,[1] and some of them affect criticality safety. Thus, the acquisition of nuclide composition and the verification of computational accuracy for fission products in MOX spent fuels are very important for shielding, criticality safety analyses, and the development of a reasonable design for spent fuel storage facilities, as well as for the introduction of burn-up credit.

A chemical isotopic analysis of actinides and fission products for PWR and BWR fuels was carried out in the ARIANE program,[2] and a comparison of the isotopic composition between the experiment and calculation has been reported as the ratios of the calculated values to the experimental ones (C/E ratios)[3,4] but their experimental composition data has not yet been published. Thus, at present, the available nuclide composition obtained experimentally and its evaluation for LWR MOX spent fuels are quite limited and insufficient, particularly in the case of high-burn-up MOX spent fuels.

In this study, a chemical isotopic analysis of a high-burn-up PWR-MOX spent fuel is carried out to determine fission product composition. Furthermore, computational analysis is carried out using the integrated burn-up calculation code system SWAT.[5] The local burn-up of fuel samples is determined by chemical isotopic analysis. The libraries used in the calculations are JENDL-3.2,[6] JENDL-3.3,[7] ENDF/B-VI.5 (release 6.5), ENDF/B-VI.8 (release 6.8),[8] JEF-2.2,[9] and JEFF-3.0,[10] which are generally used in various neutronics codes and adapted for use with SWAT. The differences between the amounts of fission products obtained by the chemical isotopic analysis and SWAT calculation are evaluated as the C/E ratios.

*Corresponding author, E-mail: sasa@criepi.denken.or.jp

Fission products, which are important as gamma and decay heat sources, neutron absorbers, or burn-up indicators and whose C/E ratios are greater than 1.05 or less than 0.95, are investigated using simplified burn-up chains. Furthermore, fission products that strongly affect the amounts of specific fission products are determined by sensitivity analysis, and the correction values for the fission yields or capture cross sections are estimated to improve the C/E ratios of specific fission products. The dependence of the C/E ratios of fission products on the type of library is also discussed using sensitivity coefficients.

II. MOX Fuels and Calculation Methods

1. Spent Fuels Used and Chemical Isotopic Analysis

Two segments with declared burn-ups of 44.5 and 45.3 MWd/kgHM were used in this study. The segments were extracted at the central part along the axial direction of two different PWR-MOX spent fuel pins (Pu enrichment: 5.07 wt.%), which were irradiated in the same fuel assembly for four cycles in the Obrigheim nuclear power reactor in Germany. The initial plutonium vector in the MOX segments was $^{238}Pu/^{239}Pu/^{240}Pu/^{241}Pu/^{242}Pu/^{241}Am = 1.50/59.00/24.38/9.34/4.85/0.94$. The average power histories and burn-ups of the segments in all cycles are given in **Table 1**.

A chemical isotopic analysis was performed on two samples, MOX1 and MOX2, at the central position of each segment. The isotopic composition of MOX1 has been reported in Ref. 11). In this study, further analysis of MOX2 was performed at the Institute for Transuranium Elements (ITU) in Karlsruhe, Germany to determine the average trend of nuclide composition in these similar MOX samples using mass and energy-based spectrometry techniques. In chemical isotopic analysis, the total dissolution of samples was performed in a nitric acid and hydrogen fluoride solution using autoclaves. Hence, in the chemical isotopic analysis, insoluble isotopes such as ruthenium dissolved in the solution. **Table 2** shows the measurement accuracy for the nuclides' determination. These values include the uncertainty in the sample preparation procedure and also in the analytical chemical technique. The times elapsed from the fuel discharge to the chemical isotopic analysis of samples MOX1 and MOX2 are given in **Table 3**.

Table 1 Average power histories and burn-ups in each cycle for high-burn-up MOX fuel segments

	Segment 1		Segment 2	
Cycle	(MW/t)	(MWd/kgHM)	(MW/t)	(MWd/kgHM)
1	31.9	9.5	32.9	9.8
2	37.0	11.9	37.9	12.2
3	38.2	12.2	38.2	12.2
4	35.5	10.9	36.2	11.1

Table 2 Measurement accuracy for nuclides determination

Nuclide	Measurement accuracy (%)
Ru, Sb, ^{134}Cs, ^{137}Cs, ^{144}Ce, ^{154}Eu	3–5
^{142}Nd, $^{145–150}Nd$	1
Rb, Sr, Y, ^{133}Cs, ^{135}Cs, La, $^{140,142}Ce$, Pr, $^{143,144}Nd$, Pm, Sm, $^{153,155}Eu$, Gd	2–3

Table 3 Elapsed times from discharge to chemical isotopic analysis

Sample	Nuclide	Period (d)
MOX1	All fission products	1636
MOX2	^{106}Ru, ^{125}Sb, ^{134}Cs, ^{137}Cs, ^{144}Ce, ^{154}Eu	2275
	Other fission products	2397

2. Calculation Method and Modeling

The nuclide composition of fission products was calculated using the SWAT code, which is an integrated burn-up code system developed at the Japan Atomic Energy Research Institute (JAERI). The code contains and combines the general-purpose neutronics codes SRAC[12] and ORIGEN-2.[13] Many infinite dilution cross sections are prepared in SWAT, and they can be updated to the effective cross sections calculated using SRAC. In this study, the neutron spectrum and the effective cross sections were calculated using the ultrafine resonance absorption calculation (PEACO) routine in SRAC, and the effective cross sections for all of the fission products evaluating their C/E ratios were calculated using PEACO. The libraries JENDL-3.2, JENDL-3.3, ENDF/B-VI.5, ENDF/B-VI.8, JEF-2.2, and JEFF-3.0, and the fission yields of JNDC-V2[14] were used in the SWAT calculation.

A square cell model was applied to the calculations, considering an equivalent volume ratio of fuel to moderator with the whole fuel assembly. The uncertainty due to the modeling of the moderator region in the square cell model was estimated, and the uncertainty in the calculated results was about 1%. The geometry used in the calculations is shown in **Fig. 1**. It is composed of three regions: fuel pellet, cladding, and moderator. The temperatures of the fuel and cladding were 900 and 600 K, respectively, and they are typical temperatures of LWR fuels. The temperature of moderator was 568 K; it is the average temperature of the inlet and outlet of coolant, corresponding to the axial positions of the samples. The constant boric acid concentration (500 ppm) was used in the calculations. The uncertainties due to temperatures, boron concentration, and depletion calculations were estimated and the uncertainty in the calculated results was about 4%. In SWAT, the neutron flux depending on the depletion is calculated using the SRAC code, which has been verified and is generally used in Japan, and burn-up calculation is carried out using the ORIGEN2

code in which the matrix exponential method is applied. Thus, in the comparison of SWAT with MVP-BURN, which is a continuous-energy Monte Carlo burn-up calculation code, the difference in their calculated results is less than 2%.[15)]

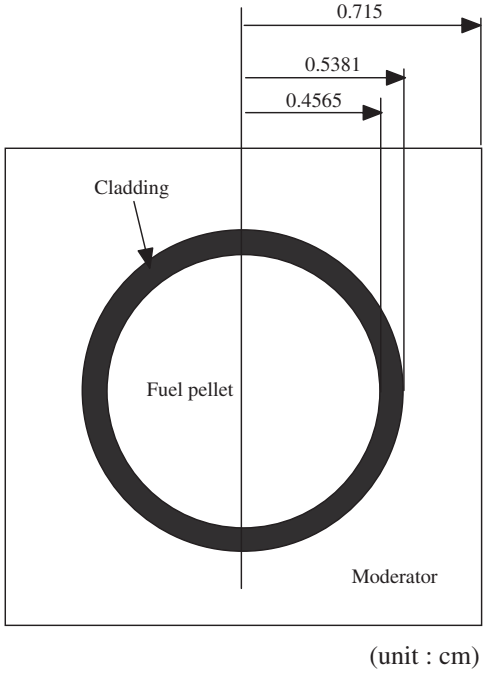

Fig. 1 Dimensions used in calculation for high-burn-up PWR-MOX

III. Results and Discussion

1. Results of Chemical Isotopic Analysis

The local burn-ups of the samples achieved in the irradiation were determined from the amounts of both total heavy metals such as uranium, neptunium, plutonium, americium, and curium isotopes, and ^{148}Nd obtained by the chemical isotopic analysis. **Table 4** shows the local burn-ups for MOX1 and MOX2 determined. The two burn-ups are quite similar. By adjusting the specific powers, the burn-ups that were equal to those determined experimentally were applied to the calculations.

The following fission products in the samples were determined by chemical isotopic analysis: rubidium (Rb), strontium (Sr), yttrium (Y), ruthenium (Ru), antimony (Sb), cesium (Cs), lanthanum (La), cerium (Ce), praseodymium (Pr), neodymium (Nd), promethium (Pm), samarium (Sm), europium (Eu), and gadolinium (Gd). **Table 5** shows the results for the number density per gram solution of the fission products obtained by the chemical isotopic analysis. The number density differs between the samples because the weights of the samples dissolved were different. Among the fission products, ^{125}Sb was analyzed only for MOX2;

Table 4 Sample burn-ups determined by chemical isotopic analysis

Sample	Burn-up (MWd/kgHM)
MOX1	46.0
MOX2	46.6

Table 5 Chemical isotopic analysis of fission products in high-burn-up PWR-MOX spent fuel

Nuclide	MOX1[11)]	MOX2	Nuclide	MOX1[11)]	MOX2
	Number/gram solution ($\times 10^{16}$)			Number/gram solution ($\times 10^{16}$)	
^{85}Rb	2.52	not measured	^{145}Nd	12.3	6.06
^{87}Rb	5.37	not measured	^{146}Nd	13.4	6.54
^{86}Sr	0.05	not measured	^{148}Nd	7.74	3.78
^{88}Sr	8.6	not measured	^{150}Nd	4.49	2.23
^{90}Sr	10.5	4.47	^{147}Pm	0.93	0.43
^{89}Y	8.89	4.22	^{147}Sm	3.99	—
^{106}Ru	0.33	0.04	^{148}Sm	3.69	—
^{125}Sb	not measured	0.02	^{149}Sm	0.09	—
^{133}Cs	27.5	15.1	^{150}Sm	6.59	—
^{134}Cs	0.81	0.20	^{151}Sm	0.39	—
^{135}Cs	16.1	8.42	^{152}Sm	2.47	—
^{137}Cs	29.0	11.3	^{154}Sm	1.21	—
^{139}La	23.6	14.4	^{153}Eu	3.24	1.75
^{140}Ce	25.6	17.6	^{154}Eu	1.51	0.26
^{142}Ce	23.0	15.2	^{155}Eu	0.12	not measured
^{144}Ce	0.12	0.01	^{154}Gd	0.39	0.20
^{141}Pr	23.8	16.1	^{155}Gd	0.12	0.14
^{142}Nd	0.41	0.23	^{156}Gd	2.78	0.92
^{143}Nd	17.8	9.43	^{158}Gd	0.66	0.15
^{144}Nd	24.1	13.0	^{160}Gd	0.04	not measured
Burn-up (MWd/kgHM)	46.0	46.6	Burn-up (MWd/kgHM)	46.0	46.6

some of the fission products such as ^{85}Rb and ^{86}Sr were analyzed only for MOX1. The results of samarium isotopes in MOX2 are excluded in Table 5 because their chemical isotopic analysis may fail.

2. Comparison of Experimental and Computational Compositions

The ratios of the calculated amounts using JENDL-3.2, JENDL-3.3, ENDF/B-VI.5, ENDF/B-VI.8, JEF-2.2, and JEFF-3.0 to the experimental ones (C/E ratios) for the fission products are shown in **Fig. 2**. The C/E ratios in the figures are averages of those of MOX1 and MOX2 because these samples were irradiated in the same fuel assembly, and their irradiation histories and burn-ups were quite similar. The C/E ratios are normalized by the residual amounts of ^{238}U, whose values are 8.57×10^{19} and 4.08×10^{19} (number/gram solution) in MOX1 and MOX2, respectively. For actinides, the C/E ratios of ^{235}U, ^{238}Pu, ^{239}Pu, ^{240}Pu, ^{241}Pu, and ^{242}Pu were 1.08, 0.96, 1.05, 1.01, 1.01, and 0.99, respectively.

In Fig. 2, the calculated ^{86}Sr amount is markedly underestimated (−85%). Regarding cesium isotopes, the calculated ^{137}Cs amounts are in agreement with the experimental ones. On the other hand, the calculated ^{134}Cs amounts are underestimated (−17%) though ^{134}Cs is important as a gamma source and is used as a relative burn-up indicator. For neodymium isotopes, the calculated amounts of ^{142}Nd, ^{143}Nd, and ^{144}Nd are underestimated, whereas those for the other neodymium isotopes are in good agreement with the experimental ones. The C/E ratio for ^{125}Sb is overestimated (about 50%). The ^{125}Sb is a metallic and insoluble species, so that its overestimation may be caused by the chemical isotopic analysis and that applying other techniques such as gamma spectrometry may be needed to obtain its accurate data. For ^{158}Gd, its C/E ratio shows a marked overestimation and there was a large difference in the C/E ratios for ^{155,156}Gd and ^{158}Gd between the samples. Therefore, this difference may be caused by the chemical isotopic analysis including the solution preparation. For the other fission products, there was scattering (−40∼70%) in the C/E ratios for ^{139}La, ^{144}Ce, ^{147}Pm, and ^{154}Eu between the samples. The scattering may be caused by the chemical isotopic analysis procedure. Thus, further acquisition of nuclide composition data of these nuclides in MOX fuels should be carried out to evaluate and discuss the calculation accuracy.

The C/E ratios for the fission products shown in **Table 6** are greater than 1.05 or less than 0.95, and their calculation accuracy is rather low, although these fission products are important gamma and decay heat sources, neutron absorbers, burn-up indicators, or relatively large amounts in spent fuels.

Table 6 Fission products investigated

Characteristics	Fission products
Gamma source/decay heat	^{90}Sr
Neutron absorption	^{133}Cs, ^{135}Cs
Burn-up indicator	^{106}Ru, ^{134}Cs
Large amount	^{88}Sr

Thus, further investigation is carried out focusing on their sensitive production paths using simplified burn-up chains in Section 4.

For europium and gadolinium isotopes, the C/E ratios for ^{154}Eu, ^{155}Eu, ^{154}Gd, ^{155}Gd, and ^{156}Gd have a large dependence on the type of library. Hence, the reason for the dependence is also discussed in Section 5.

3. Simplified Burn-up Chains of Fission Products and Sensitivity Analysis

In SWAT, many fission products can be treated in their depletion calculations. Hence, it is not convenient to focus on particular production paths for fission products. For this reason, simplified burn-up chains, in which the fission yields for short-lived fission products can be treated as cumulative fission yields, were developed as follows to investigate the fission products given in Table 6:

$$\frac{dN_i}{dt} = \gamma_i \Sigma_{f,i}\phi - \sigma_{\gamma,il}N_i\phi + \sigma_{\gamma,ji}N_j\phi - \lambda_{id}N_i + \lambda_{ni}N_n, \quad (1)$$

where $\gamma_i \Sigma_{f,i} = \gamma_{i,U235}\sigma_{f,U235}N_{U235} + \gamma_{i,U238}\sigma_{f,U238}N_{U238} + \gamma_{i,Pu239}\sigma_{f,Pu239}N_{Pu239} + \gamma_{i,Pu241}\sigma_{f,Pu241}N_{Pu241}$

$\gamma_{i,j}$: Fission yield of nuclide j to i

$\sigma_{f,i}$: One-group microscopic fission cross section of nuclide i

$\sigma_{\gamma,ij}$: One-group microscopic capture cross section of nuclide i to j

N_i: Number density of nuclide i

λ_{id}: Decay constant from nuclides i to d by β^- decay or isomeric transition

ϕ: One-group neutron flux.

In Eq. (1), one-group microscopic cross sections, the number densities of N_{U235}, N_{U238}, N_{Pu239}, and N_{Pu241} in the term $\gamma_i \Sigma_{f,i}$, and one-group neutron flux depending on burn-up were previously calculated using SWAT with JENDL-3.3. The fission yields $\gamma_{i,j}$ of the fission products were taken from the JNDC-V2 library. In this study, four simplified burn-up chains for the fission products were investigated (**Fig. 3**): (a) chain 1: ^{83}Kr–^{85}Kr, ^{85}Rb–^{87}Rb, ^{86}Sr–^{90}Sr, and ^{89}Y; (b) chain 2: ^{105}Ru–^{106}Ru; (c) chain 3: ^{131}Xe–^{135}Xe, ^{133}Cs–^{137}Cs, ^{136}Ba–^{138}Ba, and ^{139}La; (d) chain 4: ^{140}Ce–^{144}Ce, ^{141}Pr–^{143}Pr, ^{142}Nd–^{147}Nd, ^{147}Pm–^{150}Pm, ^{147}Sm–^{156}Sm, ^{153}Eu–^{156}Eu, and ^{154}Gd–^{158}Gd.

Table 7 shows the results of the comparison of nuclide composition between the simple depletion calculations with simplified burn-up chains and the SWAT calculations. The results of the two calculations agree within 2%. Hence, a sensitivity analysis followed by correction for the fission product or capture cross section was carried out using the simple depletion calculation.

Sensitivity coefficients were defined as follows.[16)]

$$S_{\sigma_{\gamma,j},Ni} = \frac{\sigma_{\gamma,j}}{N_i}\frac{\Delta N_i}{\Delta \sigma_{\gamma,j}} \quad (2)$$

$$S_{\gamma_{j,k},N_i} = \frac{\gamma_{j,k}}{N_i}\frac{\Delta N_i}{\Delta \gamma_{j,k}}, \quad (3)$$

where $S_{\sigma\gamma,j,Ni}$: Sensitivity coefficient of capture cross section of nuclide j to i

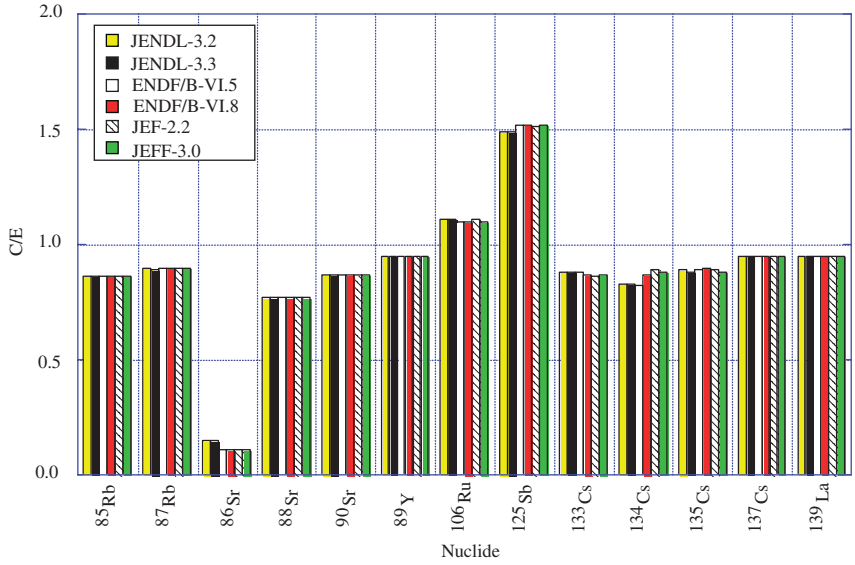

(a) ^{85}Rb–^{139}La

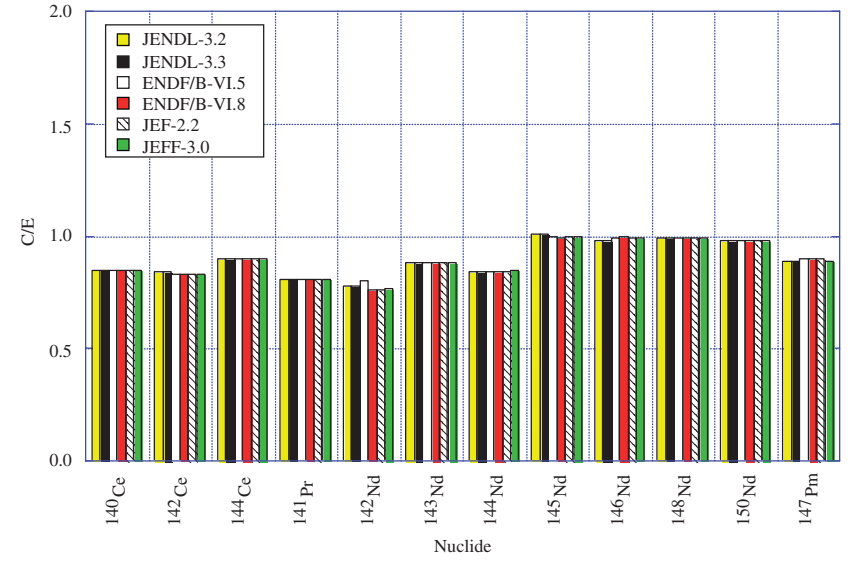

(b) ^{140}Ce–^{147}Pm

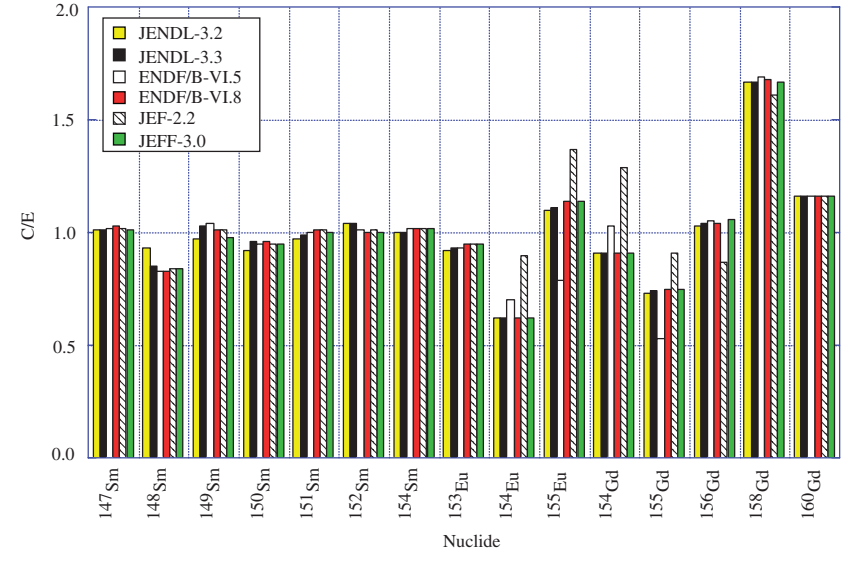

(c) ^{147}Sm–^{160}Gd

Fig. 2 Calculated and measured amounts of fission products as C/E ratios

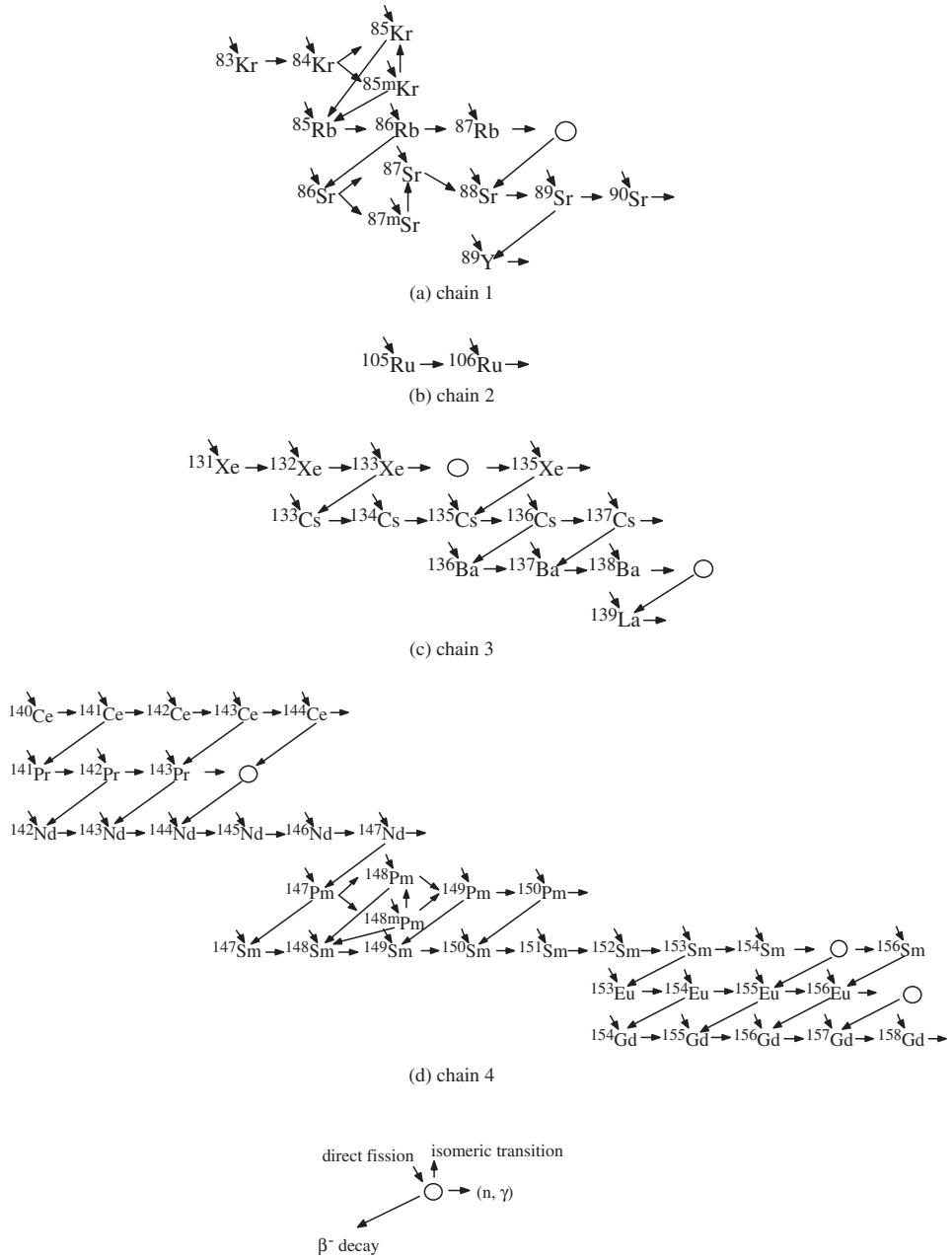

Fig. 3 Simplified burn-up chains for fission products

Table 7 Differences in amounts of fission products between simple depletion calculation and SWAT calculation with JENDL-3.3

Nuclide	Simple depletion/SWAT
^{88}Sr	1.00
^{90}Sr	1.00
^{89}Y	0.98
^{106}Ru	1.02
^{133}Cs	0.99
^{134}Cs	0.99
^{135}Cs	1.00
^{154}Eu	0.98
^{155}Eu	0.98
^{154}Gd	0.98
^{155}Gd	0.98
^{156}Gd	0.99

$S_{\gamma j,k,Ni}$: Sensitivity coefficient of fission yield for nuclide j generated by fission reaction of nuclide k to i
$\sigma_{\gamma,j}$: One-group capture cross section of nuclide j
N_i: Number density of nuclide i
$\gamma_{j,k}$: Fission yield of nuclide k to j.

In Eqs. (2) and (3), ΔN_i was estimated using Eq. (1) in which the number densities were calculated with a change by 10% in the capture cross section ($\Delta\sigma_{\gamma,j}$) and fission yield ($\Delta\gamma_{j,k}$), respectively. All of the sensitivity coefficients of the fission yields and capture cross sections that are sensitive to specific fission products discussed in the following sections are given in **Tables 8** and **9**, respectively. The main results obtained by the sensitivity analysis are as follows.

(1) Production of ^{133}Cs, ^{134}Cs, and ^{135}Cs

In the cases of ^{133}Cs and ^{134}Cs in Table 8(c), whose

Table 8 Sensitivity coefficients of fission yields for amounts of fission products

(a) Chain 1

	$S_{\gamma j,k,Ni}$											
	^{88}Sr from				^{89}Sr from				^{90}Sr form			
N_i	^{235}U	^{238}U	^{239}Pu	^{241}Pu	^{235}U	^{238}U	^{239}Pu	^{241}Pu	^{235}U	^{238}U	^{239}Pu	^{241}Pu
^{88}Sr	0.17	0.11	0.56	0.16	0.00	0.00	0.00	0.00	0.00	0.00	0.00	0.00
^{89}Sr	0.00	0.00	0.00	0.00	0.15	0.14	0.51	0.20	0.00	0.00	0.00	0.00
^{90}Sr	0.00	0.00	0.00	0.00	0.00	0.00	0.00	0.00	0.18	0.11	0.56	0.15
^{89}Y	0.00	0.00	0.00	0.00	0.18	0.12	0.55	0.14	0.00	0.00	0.00	0.00

(b) Chain 2

	$S_{\gamma j,k,Ni}$							
	^{105}Ru from				^{106}Ru from			
N_i	^{235}U	^{238}U	^{239}Pu	^{241}Pu	^{235}U	^{238}U	^{239}Pu	^{241}Pu
^{105}Ru	0.01	0.07	0.56	0.35	0.00	0.00	0.00	0.00
^{106}Ru	0.00	0.00	0.00	0.00	0.01	0.05	0.57	0.37

(c) Chain 3

	$S_{\gamma j,k,Ni}$											
	^{133}Xe from				^{134}Xe from				^{135}Xe from			
N_i	^{235}U	^{238}U	^{239}Pu	^{241}Pu	^{235}U	^{238}U	^{239}Pu	^{241}Pu	^{235}U	^{238}U	^{239}Pu	^{241}Pu
^{133}Xe	0.05	0.09	0.56	0.30	0.00	0.00	0.00	0.00	0.00	0.00	0.00	0.00
^{134}Xe	0.00	0.00	0.00	0.00	0.07	0.08	0.61	0.23	0.00	0.00	0.00	0.00
^{135}Xe	0.00	0.00	0.00	0.00	0.00	0.00	0.00	0.00	0.05	0.08	0.57	0.30
^{133}Cs	0.07	0.08	0.62	0.23	0.00	0.00	0.00	0.00	0.00	0.00	0.00	0.00
^{134}Cs	0.07	0.08	0.64	0.20	0.00	0.00	0.00	0.00	0.00	0.00	0.00	0.00
^{135}Cs	0.00	0.00	0.01	0.00	0.00	0.00	0.00	0.00	0.06	0.07	0.63	0.22
^{136}Cs	0.00	0.00	0.01	0.00	0.00	0.00	0.00	0.00	0.05	0.06	0.53	0.18
^{137}Cs	0.00	0.00	0.00	0.00	0.00	0.00	0.00	0.00	0.00	0.00	0.00	0.00

(d) Chain 4

	$S_{\gamma j,k,Ni}$															
	^{147}Nd from				^{149}Pm from				^{151}Sm from				^{152}Sm from			
N_i	^{235}U	^{238}U	^{239}Pu	^{241}Pu	^{235}U	^{238}U	^{239}Pu	^{241}Pu	^{235}U	^{238}U	^{239}Pu	^{241}Pu	^{235}U	^{238}U	^{239}Pu	^{241}Pu
^{151}Sm	0.00	0.00	0.03	0.01	0.01	0.02	0.14	0.06	0.02	0.06	0.39	0.25	0.00	0.00	0.00	0.00
^{152}Sm	0.00	0.00	0.01	0.00	0.01	0.01	0.06	0.02	0.02	0.04	0.30	0.15	0.01	0.03	0.21	0.12
^{153}Sm	0.00	0.00	0.01	0.00	0.00	0.01	0.05	0.02	0.01	0.03	0.23	0.12	0.01	0.02	0.17	0.10
^{154}Sm	0.00	0.00	0.00	0.00	0.00	0.00	0.00	0.00	0.00	0.00	0.00	0.00	0.00	0.00	0.00	0.00
^{153}Eu	0.00	0.00	0.00	0.00	0.00	0.00	0.03	0.01	0.01	0.03	0.23	0.09	0.01	0.02	0.18	0.08
^{154}Eu	0.00	0.00	0.00	0.00	0.00	0.00	0.02	0.01	0.01	0.03	0.22	0.08	0.01	0.02	0.19	0.08
^{155}Eu	0.00	0.00	0.00	0.00	0.00	0.00	0.02	0.01	0.01	0.02	0.18	0.07	0.01	0.02	0.15	0.06
^{156}Eu	0.00	0.00	0.00	0.00	0.00	0.00	0.01	0.00	0.01	0.02	0.16	0.06	0.01	0.02	0.14	0.06
^{154}Gd	0.00	0.00	0.00	0.00	0.00	0.00	0.01	0.00	0.01	0.02	0.19	0.06	0.01	0.02	0.18	0.07
^{155}Gd	0.00	0.00	0.00	0.00	0.00	0.00	0.01	0.00	0.01	0.02	0.18	0.06	0.01	0.02	0.16	0.06
^{156}Gd	0.00	0.00	0.00	0.00	0.00	0.00	0.01	0.00	0.01	0.01	0.09	0.03	0.00	0.01	0.09	0.03

(to be continued on next page)

calculated amounts are discussed in Section 4, the main production path that has large sensitivity to their amounts is

- ^{133}Xe → ^{133}Cs → ^{134}Cs.

For ^{135}Cs, from the sensitivity coefficients in Tables 8(c) and 9(b), its main sensitive production path is

- ^{135}Xe → ^{135}Cs.

(2) Production of ^{154}Eu, ^{154}Gd, ^{155}Eu, ^{155}Gd, and ^{156}Gd

For ^{154}Eu, ^{154}Gd, ^{155}Eu, ^{155}Gd, and ^{156}Gd that are discussed in Section 5, there are three sensitive production paths to their amounts as follows.

- ^{151}Sm → ^{152}Sm → ^{153}Sm → ^{153}Eu → ^{154}Eu → ^{154}Gd → ^{155}Gd
- ^{151}Sm → ^{152}Sm → ^{153}Sm → ^{153}Eu → ^{154}Eu → ^{155}Eu → ^{155}Gd
- ^{151}Sm → ^{152}Sm → ^{153}Sm → ^{153}Eu → ^{154}Eu → ^{155}Eu → ^{156}Eu → ^{156}Gd

(e) Chain 4 (cont.)

	$S_{\gamma j,k,Ni}$															
	^{153}Sm from				^{154}Sm from				^{156}Sm from				^{155}Eu from			
N_i	^{235}U	^{238}U	^{239}Pu	^{241}Pu	^{235}U	^{238}U	^{239}Pu	^{241}Pu	^{235}U	^{238}U	^{239}Pu	^{241}Pu	^{235}U	^{238}U	^{239}Pu	^{241}Pu
^{151}Sm	0.00	0.00	0.00	0.00	0.00	0.00	0.03	0.01	0.00	0.00	0.00	0.00	0.00	0.00	0.00	0.00
^{152}Sm	0.00	0.00	0.00	0.00	0.00	0.00	0.01	0.00	0.00	0.00	0.00	0.00	0.00	0.00	0.00	0.00
^{153}Sm	0.00	0.02	0.10	0.09	0.00	0.00	0.01	0.00	0.00	0.00	0.00	0.00	0.00	0.00	0.00	0.00
^{154}Sm	0.00	0.00	0.00	0.00	0.02	0.06	0.59	0.32	0.00	0.00	0.00	0.00	0.00	0.00	0.00	0.00
^{153}Eu	0.01	0.02	0.15	0.10	0.00	0.00	0.00	0.00	0.00	0.00	0.00	0.00	0.00	0.00	0.00	0.00
^{154}Eu	0.01	0.03	0.18	0.10	0.00	0.00	0.00	0.00	0.00	0.00	0.00	0.00	0.00	0.00	0.00	0.00
^{155}Eu	0.01	0.02	0.15	0.08	0.00	0.00	0.01	0.00	0.00	0.00	0.00	0.00	0.00	0.01	0.09	0.07
^{156}Eu	0.01	0.02	0.14	0.08	0.00	0.00	0.01	0.00	0.00	0.01	0.06	0.05	0.00	0.01	0.08	0.06
^{154}Gd	0.01	0.03	0.25	0.12	0.00	0.00	0.00	0.00	0.00	0.00	0.00	0.00	0.00	0.00	0.00	0.00
^{155}Gd	0.01	0.03	0.18	0.09	0.00	0.00	0.01	0.00	0.00	0.00	0.00	0.00	0.00	0.01	0.07	0.06
^{156}Gd	0.01	0.02	0.13	0.06	0.00	0.00	0.01	0.00	0.00	0.01	0.12	0.07	0.00	0.02	0.18	0.09

Table 9 Sensitivity coefficients of capture cross sections $\sigma_{\gamma,j}$ for amounts of fission products

(a) Chain 2

	$S_{\sigma\gamma,j,Ni}$	
	$\sigma_{\gamma,j}$ of	
N_i	^{105}Ru	^{106}Ru
^{105}Ru	0.00	0.00
^{106}Ru	0.00	0.00

(b) Chain 3

	$S_{\sigma\gamma,j,Ni}$				
			$\sigma_{\gamma,j}$ of		
N_i	^{132}Xe	^{135}Xe	^{133}Cs	^{134}Cs	^{135}Cs
^{133}Xe	0.01	0.00	0.00	0.00	0.00
^{134}Xe	0.00	0.00	0.00	0.00	0.00
^{135}Xe	0.00	−0.58	0.00	0.00	0.00
^{133}Cs	0.00	0.00	−0.16	0.00	0.00
^{134}Cs	0.00	0.00	0.87	−0.07	0.00
^{135}Cs	0.00	−0.49	0.02	0.02	−0.04
^{136}Cs	0.00	−0.42	0.01	0.01	0.81
^{137}Cs	0.00	0.00	0.00	0.00	0.00

(c) Chain 4

	$S_{\sigma\gamma,j,Ni}$													
								$\sigma_{\gamma,j}$ of						
N_i	^{147}Pm	^{148m}Pm	^{150}Sm	^{151}Sm	^{152}Sm	^{153}Sm	^{154}Sm	^{153}Eu	^{154}Eu	^{155}Eu	^{156}Eu	^{154}Gd	^{155}Gd	^{156}Gd
^{151}Sm	0.03	0.01	0.25	−0.92	0.00	0.00	0.00	0.00	0.00	0.00	0.00	0.00	0.00	0.00
^{152}Sm	0.01	0.01	0.11	0.02	−0.68	0.00	0.00	0.00	0.00	0.00	0.00	0.00	0.00	0.00
^{153}Sm	0.01	0.00	0.08	0.01	0.21	0.00	0.00	0.00	0.00	0.00	0.00	0.00	0.00	0.00
^{154}Sm	0.00	0.00	0.00	0.00	0.00	0.01	−0.01	0.00	0.00	0.00	0.00	0.00	0.00	0.00
^{153}Eu	0.00	0.00	0.05	0.05	0.30	0.00	0.00	−0.46	0.00	0.00	0.00	0.00	0.00	0.00
^{154}Eu	0.00	0.00	0.04	0.06	0.33	0.00	0.00	0.56	−0.67	0.00	0.00	0.00	0.00	0.00
^{155}Eu	0.00	0.00	0.03	0.05	0.27	0.00	0.01	0.48	0.24	−0.84	0.00	0.00	0.00	0.00
^{156}Eu	0.00	0.00	0.02	0.05	0.25	0.00	0.01	0.43	0.21	0.07	−0.02	0.00	0.00	0.00
^{154}Gd	0.00	0.00	0.02	0.08	0.35	0.00	0.00	0.67	−0.54	0.00	0.00	−0.08	0.00	0.00
^{155}Gd	0.00	0.00	0.02	0.06	0.29	0.00	0.01	0.52	0.10	−0.68	0.00	0.17	−0.89	0.00
^{156}Gd	0.00	0.00	0.01	0.04	0.17	0.00	0.01	0.34	0.21	0.07	−0.02	0.00	0.00	−0.05

The first production path is the main sensitive one for ^{154}Gd. In ^{155}Gd production, the sensitivity coefficient of the ^{155}Eu capture cross section to the ^{155}Gd amount is -0.68, as shown in Table 9(b), whereas that of the ^{154}Gd capture cross section to the ^{155}Gd amount is 0.17. Thus, the amount of ^{155}Gd strongly depends on that of ^{155}Eu rather than on that of ^{154}Gd. From this result, the main sensitive path for ^{155}Gd is the second one. For ^{156}Gd, the third production path, in which ^{156}Gd is mainly generated through the β^- decay of ^{156}Eu, is the main sensitive one. The sensitive coefficients of ^{156}Gd for the fission yields of ^{155}Eu are larger than those of ^{155}Eu for the fission yields of ^{155}Eu, as shown in Table 8(e). The ^{155}Eu and ^{156}Gd capture cross sections were about 400 and 4 barn, respectively. Thus, the majority of the produced ^{155}Eu amount transmuted to ^{156}Eu and then ^{156}Gd was accumulated through the β^- decay of ^{156}Eu. Consequently, the fission yields of ^{155}Eu strongly affected the accumulated ^{156}Gd amount rather than the ^{155}Eu amount and it was reflected in the sensitivity coefficients.

4. Correction of Fission Yield and Capture Cross Section on the Basis of Sensitivity Coefficient

The fission yield or capture cross section was corrected to improve the calculated amounts of fission products given in Table 6. In the correction, the fission yield or capture cross section of the fission product that strongly affects the specific fission product was corrected by making the C/E ratio for the specific fission product equal to unity using Eq. (2) or (3). Namely, the correction value for the fission yield or capture cross section was defined by Eq. (4) and estimated using the C/E ratios shown in Fig. 2 and the sensitivity coefficients listed in Tables 8 and 9.

$$\frac{R_{0,j}-R_j}{R_j}=\frac{1}{S_{j,i}}\left(\frac{1}{(C/E)_i}-1\right), \tag{4}$$

where $R_{o,j}$: Corrected capture cross section or fission yield of nuclide j
R_j: Capture cross section $\sigma_{\gamma,j}$ or fission yield $\gamma_{j,k}$ of nuclide j before correction
$S_{j,i}$: Sensitivity coefficient $S_{\sigma\gamma,j,Ni}$ or $S_{\gamma j,k,Ni}$
$(C/E)_i$: C/E ratio for nuclide i before correction.

The C/E ratios were recalculated with the correction values using Eq. (1). In the following, the $S's$ are the total of the sensitivity coefficients for the fission yields of ^{235}U, ^{238}U, ^{239}Pu, and ^{241}Pu in Table 8 or the sensitivity coefficient for the capture cross section in Table 9.

(1) ^{88}Sr and ^{90}Sr

The C/E ratios for ^{88}Sr and ^{90}Sr are 0.77 and 0.86, respectively. The amounts of ^{88}Sr and ^{90}Sr are sensitive only to their own fission yields ($S = 1.00$ for both ^{88}Sr and ^{90}Sr), not to the fission yields or capture cross sections of the other fission products in chain 1. This indicates that the underestimation of the amounts of both fission products results from the underestimation of their own fission yields. The correction value of +30% for the ^{88}Sr fission yield was estimated using Eq. (4); consequently, the C/E ratio for ^{88}Sr was improved from 0.77 to 1.00 (**Table 10**).

Similarly, for ^{90}Sr, the correction value for its own fission yield was +17%, and its C/E ratio recalculated with correction was improved from 0.86 to 1.00 (**Table 11**). The corrections for ^{88}Sr and ^{90}Sr negligibly affected the C/E ratios for the other fission products in chain 1.

(2) ^{106}Ru

The C/E ratio for ^{106}Ru is 1.13. The ^{106}Ru amount is sensitive only to ^{106}Ru's own fission yield ($S = 1.00$), as shown in Tables 8(b) and 9(a). Therefore, the overestimation of the calculated ^{106}Ru amount will result from the overestimation of ^{106}Ru's own fission yield. By using the correction value of -11% for the fission yield, the C/E ratio for ^{106}Ru was improved from 1.13 to 1.00 (**Table 12**).

(3) ^{133}Cs and ^{134}Cs

The C/E ratios for ^{133}Cs and ^{134}Cs are 0.87 and 0.83, respectively. The ^{133}Cs amount is sensitive to the ^{133}Xe fission yield ($S = 1.00$) and ^{133}Cs capture cross section ($S = -0.16$). Thus, the fission yield or capture cross section for these nuclides was corrected, and the results are shown in **Table 13**(a). The correction value of -94% for the capture cross section of ^{133}Cs resulted in a significant decrease in the C/E ratio for ^{134}Cs but an improvement in that of ^{133}Cs from 0.87 to 1.01. On the other hand, the correction value of +15% for the ^{133}Xe fission yield improved the C/E ratios for ^{133}Cs and ^{134}Cs, which were 1.00 and 0.95, respectively.

Table 10 C/E ratios of ^{88}Sr with correction

	Before correction	Correction for fission yield
		^{88}Sr +30%
Ni	C/E	C/E
^{88}Sr	0.77	1.00
^{90}Sr	0.86	0.86
^{89}Y	0.94	0.94

Table 11 C/E ratios of ^{90}Sr with correction

	Before correction	Correction for fission yield
		^{90}Sr +17%
Ni	C/E	C/E
^{88}Sr	0.77	0.77
^{90}Sr	0.86	1.00
^{89}Y	0.94	0.94

Table 12 C/E ratios of ^{106}Ru with correction

	Before correction	Correction for fission yield
		^{106}Ru −11%
Ni	C/E	C/E
^{106}Ru	1.13	1.00

Table 13 C/E ratios of ^{133}Cs and ^{134}Cs with correction

(a) C/E ratios of ^{133}Cs with correction

	Before correction	Correction for fission yield	Correction for capture cross section
		^{133}Xe +15%	^{133}Cs −94%
Ni	C/E	C/E	C/E
^{133}Cs	0.87	1.00	1.01
^{134}Cs	0.83	0.95	0.06
^{135}Cs	0.88	0.88	0.87
^{137}Cs	0.95	0.95	0.95

(b) C/E ratios of ^{134}Cs with correction

	Before correction	Correction for fission yield	Correction for capture cross section
		^{133}Xe +21%	^{133}Cs +24%
Ni	C/E	C/E	C/E
^{133}Cs	0.87	1.05	0.84
^{134}Cs	0.83	1.00	1.00
^{135}Cs	0.88	0.88	0.88
^{137}Cs	0.95	0.95	0.95

(c) C/E ratios of ^{133}Cs and ^{134}Cs with the same time correction

	Before correction	Correction for fission yield	and	Correction for capture cross section
		^{133}Xe +16%		^{133}Cs +5%
Ni	C/E	C/E		
^{133}Cs	0.87	1.00		
^{134}Cs	0.83	1.00		
^{135}Cs	0.88	0.88		
^{137}Cs	0.95	0.95		

For ^{134}Cs, its amount is highly sensitive to the ^{133}Xe fission yield ($S = 1.00$) and ^{133}Cs capture cross section ($S = 0.87$). Thus, the correction was carried out on the fission yield or capture cross section of the two fission products. The correction value of +24% for the capture cross section of ^{133}Cs resulted in a decrease in the C/E ratio for ^{133}Cs but an improvement in that for ^{134}Cs from 0.83 to 1.00. On the other hand, the correction value of +21% for the ^{133}Xe fission yield improved the C/E ratios for ^{134}Cs and ^{133}Cs (Table 13(b)). From the trend of the C/E ratio for each of ^{133}Cs and ^{134}Cs, the corrections for ^{133}Xe and ^{133}Cs were performed at the same time. Table 13(c) shows the results. The correction values of +16% and +5% for the ^{133}Xe fission yield and ^{133}Cs capture cross section, respectively, improved the C/E ratios simultaneously for ^{133}Cs and ^{134}Cs. This result suggests that the underestimation of the calculated amounts of ^{133}Cs and ^{134}Cs mainly results from the underestimation of the ^{133}Xe fission yield and additionally, the underestimation of the ^{133}Cs capture cross section.

(4) ^{135}Cs

The C/E ratio for ^{135}Cs is 0.88. The ^{135}Cs amount is highly sensitive to the fission yield and capture cross section of ^{135}Xe ($S = -0.98$ and $S = -0.49$, respectively). By using the correction value of +14% for the ^{135}Xe fission yield, the C/E ratio for ^{135}Cs was improved to 1.00, and the correction value of −28% for the ^{135}Xe capture cross section also improved the C/E ratio for ^{135}Cs to 1.03 (**Table 14**). These corrections hardly affected the C/E ratios for the other fission products. Thus, these results suggest that the underestimation of the fission yield or the overestimation of the capture cross section of ^{135}Xe mainly results in the underestimation of the calculated ^{135}Cs amount.

5. Comparison of JENDL with ENDF/B, JEF, and JEFF for Fission Products Showing Large Dependence on Type of Library

Among the fission products shown in Fig. 2, the C/E ratios for ^{154}Eu, ^{155}Eu, ^{154}Gd, ^{155}Gd, and ^{156}Gd strongly depend on the type of library. The reason for this dependence was therefore investigated using sensitivity coefficients as follows.

(1) ^{154}Eu and ^{154}Gd

The C/E ratios for ^{154}Eu and ^{154}Gd calculated with ENDF/B-VI.5 and JEF-2.2 are greater than those calculated with the other libraries. In the main sensitive path for ^{154}Eu described in Section 3, the capture cross sections of ^{152}Sm and ^{153}Eu, and the C/E ratios for ^{151}Sm to ^{153}Eu isotopes

Table 14 C/E ratios of ^{135}Cs with correction

	Before correction	Correction for fission yield	Correction for capture cross section
		^{135}Xe +14%	^{135}Xe −28%
Ni	C/E	C/E	C/E
^{133}Cs	0.87	0.87	0.87
^{134}Cs	0.83	0.83	0.83
^{135}Cs	0.88	1.00	1.03
^{137}Cs	0.95	0.95	0.95

are similar regardless of the type of library used though the ^{154}Eu amount is particularly sensitive to the capture cross sections of ^{152}Sm and ^{153}Eu. Additionally, the ^{154}Eu capture cross sections in ENDF/B-VI.5 and JEF-2.2 are about 93 and 68 barn, respectively. These values are smaller than those in the other libraries (about 105 barn). The ^{154}Eu amount is also sensitive to ^{154}Eu's own capture cross section ($S = -0.67$). Thus, the relative larger amount of ^{154}Eu calculated with the two libraries was caused by the small capture cross section of ^{154}Eu. Consequently, the calculated amount of ^{154}Gd reflected that of ^{154}Eu depending on the type of library. In the new libraries ENDF/B-VI.8 and JEFF-3.0, the capture cross sections for ^{154}Eu were close to those in the other libraries.

(2) ^{155}Eu, ^{155}Gd, and ^{156}Gd

In the main sensitive path for ^{155}Gd mentioned in Section 3, the C/E ratios for ^{155}Eu and ^{155}Gd calculated with ENDF/B-VI.5 are smaller than those calculated with the other libraries. The capture cross section of ^{154}Eu in ENDF/B-VI.5 is smaller than those in the other libraries, except for JEF-2.2, and the capture cross section of ^{155}Eu in ENDF/B-VI.5 (about 640 barn) is larger than those in the other libraries (230–450 barn). Additionally, the ^{155}Eu amount is sensitive to ^{154}Eu and ^{155}Eu's own capture cross sections. The ^{155}Eu amount calculated with ENDF/B-VI.5 was therefore smaller than those calculated with the other libraries; in turn, the calculated amount of ^{155}Gd also reflected that of ^{155}Eu. The capture cross section for ^{155}Eu in ENDF/B-VI.8 was close to those in JENDL and JEFF-3.0.

In the calculation with JEF-2.2, the capture cross section of ^{155}Eu (230 barn) is smaller than those calculated with the other libraries (430–640 barn). Thus, the C/E ratio for ^{155}Eu in JEF-2.2 was greater than those in the other libraries; consequently, the C/E ratio for ^{155}Gd reflected that for ^{155}Eu. The smaller capture cross section of ^{155}Eu also suppressed the ^{156}Gd calculated amount; consequently, the C/E ratio for ^{156}Gd was smaller than those calculated with the other libraries.

IV. Conclusions

A chemical isotopic analysis of a high-burn-up PWR-MOX spent fuel was carried out. Furthermore, computational analysis was carried out using the integrated burn-up calculation code system SWAT. The libraries used in this study were JENDL-3.2, JENDL-3.3, ENDF/B-VI.5, ENDF/B-VI.8, JEF-2.2, and JEFF-3.0 adapted to the SWAT code. The difference between the amounts of fission products obtained by the chemical isotopic analysis and SWAT calculation was evaluated as the C/E ratios. A sensitivity analysis of the fission products ^{88}Sr, ^{90}Sr, ^{106}Ru, ^{133}Cs, ^{134}Cs, and ^{135}Cs was carried out to improve their C/E ratios using the simple depletion calculation with simplified burn-up chains, and the correction values for the fission yields or capture cross sections were estimated to improve the C/E ratios. The dependence of the C/E ratios for the fission products on the type of library was also investigated. The following results were obtained.

(1) The isotopic compositions of rubidium, strontium, yttrium, ruthenium, antimony, cesium, lanthanum, cerium, praseodymium, neodymium, promethium, samarium, europium, and gadolinium were determined experimentally to accumulate the nuclide composition, as well as to evaluate and improve the calculation accuracy.

(2) For ^{88}Sr, ^{90}Sr, and ^{106}Ru, the correction for their own fission yields significantly improved their C/E ratios. For ^{133}Cs and ^{134}Cs, the corrections for the fission yield of ^{133}Xe and the capture cross section of ^{133}Cs improved their C/E ratios. For ^{135}Cs, its calculated amount was highly sensitive to the fission yield and capture cross section of ^{135}Xe. Thus, the correction for the fission yield or capture cross section of ^{135}Xe markedly improved the C/E ratio for ^{135}Cs.

(3) For ^{154}Eu and ^{154}Gd calculated with ENDF/B-VI.5 and JEF-2.2, the relatively larger amount of ^{154}Eu calculated with these two libraries resulted from ^{154}Eu's own small capture cross section; consequently, the calculated amount of ^{154}Gd also reflected that of ^{154}Eu. In the cases of ^{155}Eu and ^{155}Gd calculated with ENDF/B-VI.5, the capture cross section of ^{154}Eu was smaller than those in the other libraries; in contrast, that of ^{155}Eu was larger than those in the other libraries. The ^{155}Eu amount calculated with ENDF/B-VI.5 was therefore smaller than those calculated with the other libraries; in turn, the calculated amount of ^{155}Gd also reflected that of ^{155}Eu. In the calculation with JEF-2.2, the capture cross sections of ^{155}Eu are smaller than those in the calculation with the other libraries. Thus, the calculated ^{155}Eu amount with JEF-2.2 is greater than those with the other libraries; consequently, the calculated amount of ^{155}Gd reflected that of ^{155}Eu. The smaller capture cross section

of ^{155}Eu calculated with JEF-2.2 also suppressed the ^{156}Gd calculated amount.

Regarding the acquisition of nuclide composition, additional composition data for ^{139}La, ^{144}Ce, ^{147}Pm, ^{154}Eu, and gadolinium isotopes are required to advance the evaluation because they are important neutron absorption nuclides or burn-up indicators. Among neodymium isotopes, it is necessary to evaluate the calculation accuracy for ^{142}Nd and ^{143}Nd, which are neutron absorption nuclides.

Acknowledgement

The chemical isotopic analysis in this study was carried out under contract with the Ministry of Economy, Trade and Industry (METI) of the Japanese government.

References

1) Atomic Energy Society of Japan, *Advances in Nuclear Fuel Technology —Present and Future—*, 332 (2001), [in Japanese].
2) M. Lippens, D. Boulanger, J. Basselier *et al.*, "Source term assessment: ARIANE programme," *ICEM'01 8th Int. Conf. on Radioactive Waste Management and Environment Remediation*, Sep. 30–Oct. 4, 2001, Brugge, Belgium (2001).
3) B. D. Murphy, R. T. Primm III, "Simulation of mixed-oxide and low-enriched uranium fuel burnup in a pressurized water reactor and validation against destructive analysis results," *Nucl. Sci. Eng.*, **142**, 258–269 (2002).
4) Y. Ando, K. Yoshioka, I. Mitsuhashi *et al.*, "Development and verification of Monte Carlo burnup calculation system," *Proc. 7th Int. Conf. on Nuclear Criticality Safety (ICNC2003)*, Oct. 20–24, 2003, Tokai-mura, Japan, JAERI-Conf 2003-019, Japan Atomic Energy Research Institute, 494–499 (2003).
5) K. Suyama, T. Kiyosumi, H. Mochizuki, *Revised SWAT–The Integrated Burn-up Calculation Code System*, JAERI-Data/Code 2000-027, Japan Atomic Energy Research Institute (JAERI), (2000), [in Japanese].
6) T. Nakagawa, K. Shibata, S. Chiba *et al.*, "Japanese Evaluated Nuclear Data Library Version 3 Revision-2: JENDL-3.2," *J. Nucl. Sci. Technol.*, **32**, 1259 (1995).
7) K. Shibata, T. Kawano, T. Nakagawa *et al.*, "Japanese Evaluated Nuclear Data Library Version 3 Revision-3: JENDL-3.3," *J. Nucl. Sci. Technol.*, **39**, 1125 (2002).
8) P. F. Rose, *ENDF-201, ENDF/B-VI Summary Documentation*, BNL-NCS-17541, 4th Edition, Brookhaven National Laboratory (BNL), (1991).
9) C. Nordborg, M. Salvatores, "Status of the JEF Evaluated Data Library," *Proc. Int. Conf. on Nuclear Data for Science and Technology*, Gatlinburg, Tennessee, USA, May 9–13, 1994, Vol. 2, 680 (1994).
10) R. Jacqmin, R. Forrest, J. Rowlands *et al.*, "Status of the JEFF-3 Project," *Proc. Int. Conf. on Nuclear Data for Science and Technology*, Tsukuba, Japan, Oct. 7–12, 2001, Vol. 1, 54 (2002).
11) A. Sasahara, T. Matsumura, G. Nicolaou, *Post Irradiation Examinations and the Validity of Computational Analysis for High Burn-up UO_2 and MOX Spent Fuels*, CRIEPI report, T95012, (1996), [in Japanese].
12) K. Tsuchihashi, Y. Ishiguro, K. Kaneko, M. Ido, *Revised SRAC Code System*, JAERI 1302, Japan Atomic Energy Research Institute (JAERI), (1986), [in Japanese].
13) A. G. Croff, *A User's Manual for the ORIGEN2 Computer Code*, ORNL/TM-7175, Oak Ridge National Laboratory (1980).
14) K. Tasaka, J. Katakura, H. Ihara *et al.*, *JNDC Nuclear Data Library of Fission Products —second version—*, JAERI 1320, Japan Atomic Energy Research Institute (JAERI), (1990).
15) K. Okumura, S. Ohki, M. Yamamoto *et al.*, *Study on the Prediction Accuracy of Nuclide Generation and Depletion with JENDL*, JAERI-Research 2004-025, Japan Atomic Energy Research Institute, (2005), [in Japanese].
16) K. Kobayashi, *Reactor Physics*, Corona Publishing Co., Ltd., (1996), [in Japanese].